Journal of Aerospace Science and Technology 1 (2016) 7-12
doi: 10.17265/2332-8258/2016.01.002

Identification of Continuous-Time Linear Aircraft Models Using Subspace Identification

Atsushi Fujimori
Department of Mechanical Engineering, University of Yamanashi, Kofu, Yamanashi 400-8511, Japan

Abstract: This paper considers the possibility of estimating continuous-time linear aircraft models by using the subspace identification. The outline of the subspace identification for estimating the continuous-time linear model is first mentioned. The identification simulation in which the subspace identification is then applied to the modeling of aircraft in the lateral motion is performed. As a result, the continuous-time linear aircraft model is appropriately estimated by the subspace identification if the amount of the measurement noise is not so much.

Key words: Subspace identification, aircraft model, aerodynamic derivatives.

1. Introduction

Modeling of aircraft is one of important design process for constructing flight control systems. This paper presents a modeling technique for aircraft based on the subspace identification. The subspace identification is to estimate the state-space matrices of the system to be identified based on the realization theory and is one of powerful system identification approaches [1, 2]. There has been few application of subspace identification to the modeling of aircraft. This paper then considers the possibility of the subspace identification as a technique for obtaining continuous-time linear aircraft models. The benefits of subspace identification are given as follows: (i) there is no modifications on the procedure for application to multi-input and multi-output systems, (ii) it is not so hard to determine the order of model through the singular value decomposition in the subspace identification calculation. On the other hand, since the subspace identification is to identify a discrete-time model, the transformation from the discrete-time to the continuous-time, called the inverse transformation in this paper, is performed to obtain the continuous-time model. Then, alias elements may appear in the obtained continuous-time model. If the bandwidth of the modes included in the system to be identified is known in advance, alias elements are suppressed by giving the sampling frequency which is sufficiently larger than the bandwidth. As another point to be taken into consideration, the state variables of the model estimated by the subspace identification are not generally related to the physical variables of the system to be identified. To estimate the physical parameters in the system, the state variables of the estimated model have to be transformed into those of the corresponding physical system. If these manipulations can be performed, the subspace identification is applicable to modeling of aircraft.

Linear aircraft models are generally composed by the characteristic dynamic modes [3], whose natural frequencies are roughly estimated from the frequency response. Furthermore, it is not unusual that all physical state variables can be obtained in the measurement systems of aircraft. Thus, the necessary conditions for application of the subspace identification have been arranged in aircraft modeling. This paper first presents the outline of the subspace identification for estimating the continuous-time linear aircraft model. The identification simulation in which the subspace

Corresponding author: Atsushi Fujimori, Ph.D., research field: flight control design.

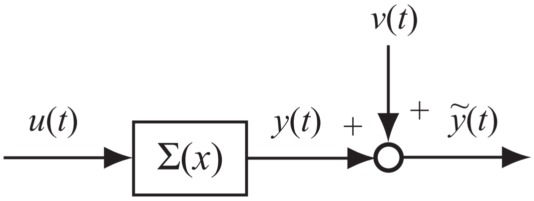

Fig. 1 An identification system.

identification is then applied to the modeling of aircraft in lateral motion is performed. The effectiveness of the proposed technique is discussed in the identification simulation.

2. Identification of Continuous-Time Linear Model by Subspace Identification

This section describes the procedures of identifying the continuous-time LTI (linear time-invariant) system by the subspace identification. Since the subspace identification method used in this paper is standard such as N4SID, MOESP, the details of the subspace identification methods are referred in [1, 2].

A system to be identified is given by the following LTI system

$$\Sigma(x): \begin{cases} \dot{x}(t) = Ax(t) + Bu(t) \\ y(t) = Cx(t) + Du(t) \end{cases} \tag{1}$$

where, t is the continuous-time. $u(t) \in R^m$ is the input, $y(t) \in R^p$ is the output and $x(t) \in R^n$ is the state vectors, respectively. The measurable output is given by

$$\tilde{y}(t) = y(t) + v(t) \tag{2}$$

where, $v(t) \in R^p$ is the measurement noise (Fig. 1). In this paper, it is assumed in Eq. (1) that

$$y(t) = x(t) \tag{3}$$

That is, all state variables are measurable. Eq. (3) indicates

$$C = I_n, \quad D = 0 \tag{4}$$

Then, the objective of system identification in this paper is to estimate matrices A and B in Eq. (1) as accurately as possible.

The rest of this section shows the identification procedures. For identification, the following N+1 paired input and the measured output signals which are obtained with a constant sampling time T_s are used.

$$\{u(t), \tilde{y}(t)\} \qquad (t = 0, T_s, \cdots, NT_s) \tag{5}$$

For convenience hereafter, the discrete-time input which is obtained by sampling $u(t)$ at $t = kT_s$ is written as:

$$u[k] = u(kT_s) \qquad (k = 0, 1, 2, \cdots) \tag{6}$$

Other discrete-time signals are similarly denoted.

Step 1: Using N+1 paired input and the measured output signals (5), the following discrete-time LTI model is estimated by a subspace identification method.

$$\begin{cases} z[k+1] = A_d z[k] + B_d u[k] \\ y[k] = C_d z[k] \end{cases} \tag{7}$$

where, $z[k] \in R^n$ is the state vector which is defined by the identification.

Step 2: When Eq. (7) is regarded as a discrete-time LTI model with the zero-th order hold, the continuous-time LTI model is inversely transformed into:

$$\begin{cases} \dot{z}(t) = A_c z(t) + B_c u(t) \\ y(t) = C_c z(t) \end{cases} \tag{8}$$

where,

$$\begin{bmatrix} A_c & B_c \\ 0 & 0 \end{bmatrix} = \frac{1}{T_s} \ln \begin{bmatrix} A_d & B_d \\ 0 & I_m \end{bmatrix}, \tag{9}$$

$$C_c = C_d \tag{10}$$

Step 3: From Eq. (3), we have:

$$y(t) = x(t) = C_c z(t) \tag{11}$$

If C_c is nonsingular, Eq. (8) is transformed into:

$$\begin{cases} \dot{x}(t) = C_c A_c C_c^{-1} x(t) + C_c B_c u(t) \\ y(t) = x(t) \end{cases} \tag{12}$$

Remark 1: It should be noted that the model estimated in Step 1 must be strictly proper to keep Eq. (4). The definition of z is varied every identification calculation. Although you can use other hold assumption in Step 2, there are no advantages of others over the zero-th order hold. Moreover, to suppress alias elements due to the inverse transformation in Step 3 as small as possible, the sampling time T_s should be selected so that the Nyquist frequency is sufficiently larger than the natural frequencies of the identified system [4]; that is,

$$T_s \ll \frac{\pi}{\rho(A)} \tag{13}$$

where, $\rho(A)$ is the spectral radius of A. If C_c is singular, return to Step 1 and a discrete-time model is re-estimated by the subspace identification. In identification simulation which will be shown in the following section, there is few cases that C_c is singular.

3. Identification Simulation of Aircraft Model

This section shows the identification simulation of the continuous-time lateral linear aircraft model using the subspace identification. The state-space equation of the lateral motion of aircraft is first shown. The evaluation indexes used in this paper are given. The identification results are then shown.

3.1 Lateral Model

The state-space equation of the lateral motion of aircraft is given by Ref. [3],

$$\dot{x}_{lat}(t) = A_{lat}x_{lat}(t) + B_{lat}u_{lat}(t) \tag{14}$$

where,

$$x_{lat} = [\beta \quad p \quad r \quad \varphi]^T, \quad u_{lat} = [\delta_a \quad \delta_r]^T \tag{15}$$

The state vector x_{lat} consists of the sideslip angle β, the roll rate p, the yaw rate r and the roll angle φ. The input vector u_{lat} consists of the aileron deflection angle δ_a and the rudder deflection angle δ_r. Matrices A_{lat} and B_{lat} are given by:

$$A_{lat} = E_{lat}^{-1}M_{lat}, \quad B_{lat} = E_{lat}^{-1}L_{lat} \tag{16}$$

where,

$$M_{lat} = \begin{bmatrix} Y_\beta & Y_p & Y_r - U_0 & g \\ L_\beta & L_p & L_r & 0 \\ N_\beta & N_p & N_r & 0 \\ 0 & 1 & 0 & 0 \end{bmatrix}, L_{lat} = \begin{bmatrix} Y_{\delta_a} & Y_{\delta_r} \\ L_{\delta_a} & L_{\delta_r} \\ N_{\delta_a} & N_{\delta_r} \\ 0 & 0 \end{bmatrix},$$

$$E_{lat} = \begin{bmatrix} U_0 & 0 & 0 & 0 \\ 0 & 1 & -I_{xz}/I_{xx} & 0 \\ 0 & -I_{zx}/I_{zz} & 1 & 0 \\ 0 & 1 & 0 & 1 \end{bmatrix} \tag{17}$$

In matrices L_{lat} and M_{lat}, Y_β, Y_p, … are the aerodynamic derivatives of the lateral model in the frame of the stability axis. U_0 is the steady-state flight velocity. Furthermore, in matrices E_{lat}, I_{xx} and I_{zz} are the moments of inertia and I_{xz} (= I_{zx}) is the product of inertia.

There are three kinds of characteristic modes in the lateral model (14); the spiral mode denoted as "*S*", the roll mode "*R*" and the Dutch roll mode "*D*", respectively. Since these modes are strongly coupled with each other, almost all of the aerodynamic derivatives in the lateral model are related these three modes [3].

3.2 Evaluation Indexes

It is desirable that the identification results are evaluated from the several points of view. This paper uses the following indexes.

(I-1) Multiplicative error of aerodynamic derivative: Let the true and the estimated values of the aerodynamic derivative Y_β be Y_β^* and $\hat{Y}_\beta$, respectively. If $Y_\beta^* \neq 0$, the multiplicative error is defined as

$$Er(Y_\beta) = \left| \frac{\hat{Y}_\beta - Y_\beta^*}{Y_\beta^*} \right| \times 100\% \tag{18}$$

The multiplicative errors of other derivatives are similarly defined.

(I-2) Error of characteristic mode: Let the characteristic mode be denoted as $\lambda_\#$ where # is given by $\# \in \{S, R, D\}$. Letting the true and the estimated values of characteristic mode $\lambda_\#$ be $\lambda_\#^*$ and $\hat{\lambda}_\#$, respectively, the error of characteristic mode is then defined as:

$$\varepsilon(\lambda_\#) = \left|\hat{\lambda}_\# - \lambda_\#^*\right| \tag{19}$$

(I-3) ν-gap metric: Let the transfer functions of the true and the estimated continuous-time linear models be $P^*(s)$ and $\hat{P}(s)$, respectively, where s is the Laplace operator. The ν-gap metric is defined as Ref. [5]

$$\delta_\nu = \sup_\omega \kappa(\hat{P}(j\omega), P^*(j\omega)) \tag{20}$$

where,

$$\kappa(X,Y) = \bar{\sigma}[(I + Y\bar{Y})^{-1/2}(Y - X)(I + X\bar{X})^{-1/2}]$$

$\bar{X}(s)$ means the conjugate transfer function of $X(s)$ and $\bar{\sigma}$ means the maximum singular value.

Remark 2: Index (I-1) evaluates the estimated aerodynamic derivatives which are included in the aircraft model. That is, (I-1) is a local evaluation index of the estimated model. Index (I-2) is the difference of the characteristic mode between the estimated and the true models in the complex-plane. Index (I-3) means a model error evaluated in the frequency region. The range of the δ_ν is normalized as $0 \le \delta_\nu \le 1$. δ_ν is essentially derived from the robust stability condition based on the normalized coprime factorization [5]. Letting $K(s)$ be the transfer function of a continuous-time controller which is designed by using the estimated model $\hat{P}(s)$, the robust stability condition that $K(s)$ stabilizes the true model $P^*(s)$ is given by

$$\delta_\nu < b_K \tag{21}$$

where, b_K is the normalized stability margin ($0 \le b_K \le 1$) [5]. Satisfying Eq. (21) means that not only $K(s)$ stabilizes $P^*(s)$ but also $\hat{P}(s)$ is valid for control design.

3.3 Simulation Results

The aircraft to be identified was referred from Ref. [6]. The true values of the lateral aerodynamic derivatives used in identification simulation are given by Table 1. The flight condition was given by the level flight whose flight velocity was U_0 = 100 m/s. The input for exciting the aircraft was given by the white random signal whose amplitude was $|\delta_a|$, $|\delta_r| < 3$ deg. The subspace identification method used was N4SID method [1, 2]. The sampling time was given by T_s = 0.01 s and the number of data was N = 1,000.

As an index for defining the amount of the noise, this paper adopts the NSR (noise signal ratio) which is defined as follows.

$$\text{NSR} = \frac{\| v_s \|}{\| y_s \|} \times 100\% \tag{22}$$

where, $s \in \{1, \ldots, p\}$, the norm in Eq. (22) means the Euclid norm of the sampling vector which consists of N+1 sampled data. That is, NSR in Eq. (22) indicates the amplitude ratio between the measurement noise and the true output. In this paper, y_s of the lateral model was given by the side slip angle β. v_s was given by the white noise.

Figs. 2-4 show the identification results where NSR was given by NSR ≈ 50%. The random responses (Fig. 2) and the frequency responses (Fig. 3) of the estimated models almost approximated those of the true models. The poles of the estimated models were located near those of the true models (Fig. 4).

Figs. 5-7 show the identification results where NSR was given in the range of 0 ≤ NSR < 90% by approximately 10% interval. Fig. 5 shows the multiplicative error Er of the lateral aerodynamic derivatives. Fig. 6 shows the error of characteristic

Table 1 Aerodynamic derivative in lateral model of aircraft.

Y_β	Y_p	Y_r	L_β	L_p	L_r	N_β	N_p	N_r	$Y_{\delta a}$	$Y_{\delta r}$	$L_{\delta a}$	$L_{\delta r}$	$N_{\delta a}$	$N_{\delta r}$
-15.566	0	0.835	-1.874	-0.971	0.264	1.061	-0.089	-0.211	0	3.139	4.540	0.417	0	-0.720

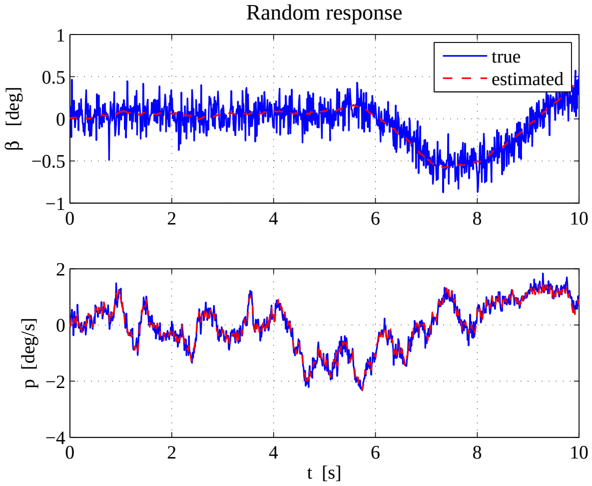

Fig. 2 Random responses of *β* and *p* where NSR ≈ 50%.

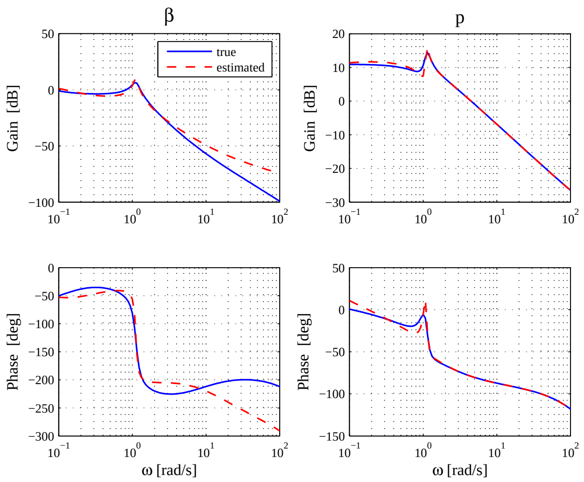

Fig. 3 Frequency responses of lateral model where NSR ≈ 50%.

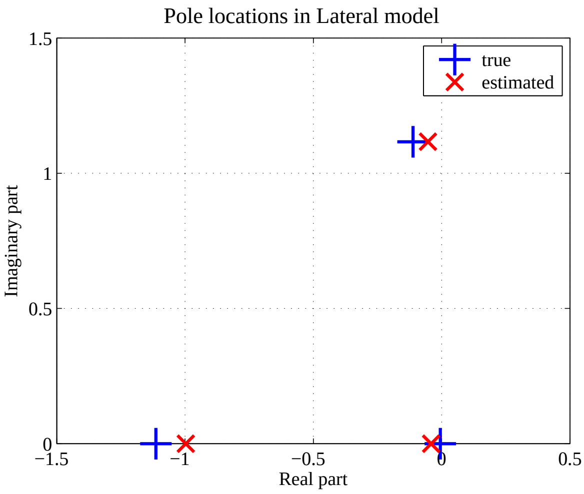

Fig. 4 Pole location of lateral model where NSR ≈ 50%.

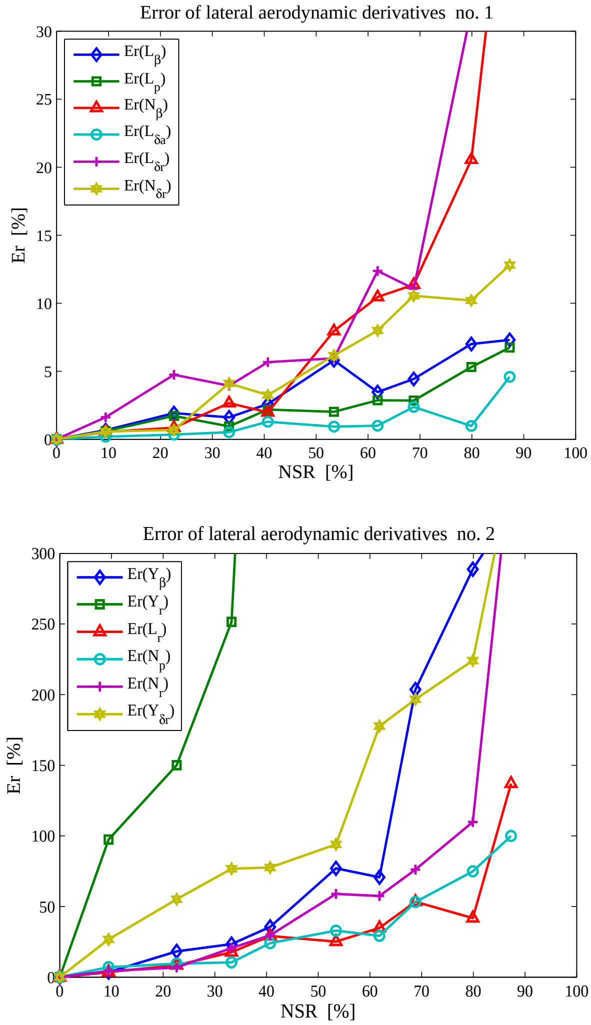

Fig. 5 Error of lateral aerodynamic derivatives.

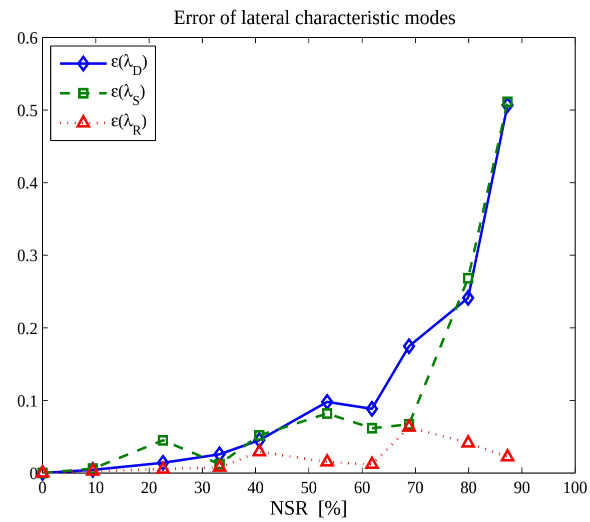

Fig. 6 Pole location of lateral model where NSR ≈ 50%.

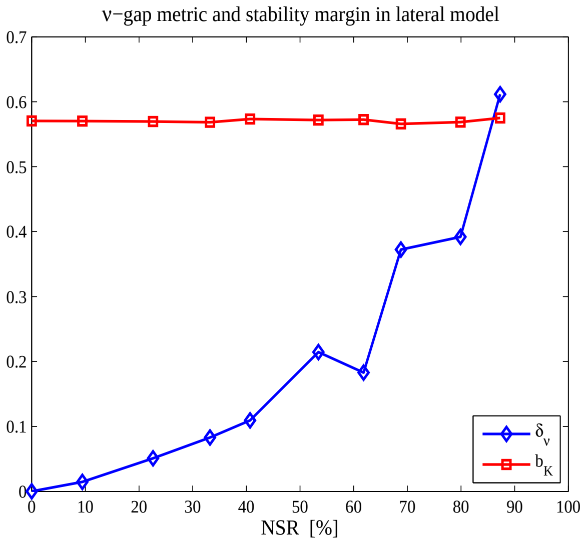

Fig. 7 *v*-gap metric and stability margin in lateral model.

modes $\varepsilon(\lambda_{\#})$ of the lateral models. The upper figure in Fig. 5 shows the aerodynamic derivatives whose *Er* was less than 40% in the examined range, while the lower figure shows the others. Although there were some derivatives whose *Er* was large in the region of NSR<30%, the error of the characteristic mode in this region was not so large (Fig. 6). That is, these derivatives were not sensitive to the characteristic modes. The error of the characteristic modes was increased slowly in the region of NSR < 50% but steeply over the region.

Fig. 7 shows the *v*-gap metric δ_v with respect to NSR. According to the increase of NSR, δ_v was increased to 0.612. Fig. 7 also shows the stability margin b_K [5] in which the estimated models were used to design an LQR state-feedback law. b_K was obtained as $b_K \approx 0.57$ for the examined range of NSR. That is, the robust stability condition (21) was satisfied in the region of NSR < 85%.

Summarizing the identification simulation, the characteristic modes and the *v*-gap metric of lateral linear aircraft models were not so varied under the presence of the measurement noise although there were some aerodynamic derivatives whose multiplicative error was large. It is concluded that the continuous-time linear aircraft model was appropriately estimated by the subspace identification in the region of NSR < 50%.

4. Concluding Remarks

This paper has considered the possibility of estimating continuous-time lateral linear aircraft models by using the subspace identification. The continuous-time linear aircraft model was appropriately estimated by the subspace identification if the amount of the measurement noise was not so much. This paper treated the white random signal as the measurement noise. When the noise is colored, it is possible to suppress the estimation bias due to the colored measurement noise by using subspace identification methods such as PI-MOESP or PO-MOESP [1, 2] in Step 1. The identification simulation for the colored noise is also similar to that for the white noise as shown in this paper.

References

[1] Verhaegen, M., and Verdult, V. 2007. *Filtering and System Identification—A Least Square Approach.* Cambridge University Press.

[2] Overschee, P., and Moor, B. 1996. *Subspace Identification for Linear Systems*. Kluwer Academic Publishers.

[3] Schmit, L. V. 1998. *Introduction to Aircraft Dynamics*. AIAA.

[4] Feuer, A., and Goodwin, G. C. 1996. *Sampling in Digital Signal Processing and Control*. Birkhauser.

[5] Vinnicombe, G. 2001. *Uncertainty and Feedback (H_inf Loop-Shaping and the V-Gap Metric)*. Imperial College Press.

[6] Isozaki, K., Masuda, K., Taniuchi, A., and Watari, M. 1980. "Flight Test Evaluation of Variable Stability Airplane." *KHI. Tech. Rev.* 75: 50-8.